Geophysical Research Letters

RESEARCH LETTER
10.1029/2020GL090851

Emerging Pacific Quasi-Decadal Oscillation Over the Past 70 Years

Jin Chunhan[1], **Wang Bin**[2,3], **and Liu Jian**[1,4]

[1]Key Laboratory for Virtual Geographic Environment of Ministry of Education/State Key Laboratory Cultivation Base of Geographical Environment Evolution of Jiangsu Province and Jiangsu Center for Collaborative Innovation in Geographical Information Resource Development and Application, School of Geography Science, Nanjing Normal University, Nanjing, China, [2]Department of Atmospheric Sciences and International Pacific Research Center, School of Ocean and Earth Science and Technology, University of Hawaii at Manoa, Honolulu, HI, USA, [3]Earth System Modeling Center, Nanjing University of Information Science and Technology, Nanjing, China, [4]School of Mathematical Science, Jiangsu Provincial Key Laboratory for Numerical Simulation of Large Scale Complex Systems, Nanjing Normal University, Nanjing, China

Key Points:

- Equatorial central Pacific's Sea surface temperature exhibits a conspicuous quasi-decadal oscillation (QDO) since 1951 but not before
- The evolution of QDO warming involves a sequence of air-sea interaction mechanisms in the subtropical Pacific and the equatorial Pacific
- The QDO follows the 11-year solar cycle with a 1-to-2-year phase delay and potentially links to the nonlinear behavior of ENSO

Supporting Information:

- Supporting Information S1

Correspondence to:
J. Liu,
jliu@njnu.edu.cn

Citation:
Chunhan, J., Bin, W., & Jian, L. (2021). Emerging Pacific Quasi-Decadal Oscillation over the past 70 years. *Geophysical Research Letters*, *48*, e2020GL090851. https://doi.org/10.1029/2020GL090851

Received 16 SEP 2020
Accepted 27 NOV 2020

Abstract Quasi-decadal variation in various Pacific regions has been recognized for decades but its spatial-temporal characteristics and generation mechanisms remain poorly understood. Here we show that the sea surface temperature (SST) in the equatorial central Pacific (ECP) exhibits a prominent 11-year periodicity since 1951 but not before. An episodic-like quasi-decadal warm event is initiated in a northeast-southwest tilted belt from the United States' west coast to the ECP. The initial development involves positive feedback between atmospheric heating-induced Rossby waves and underlying SST in the tropical North Pacific. The amplification of ECP warming is primarily due to equatorward heat advection and deepening thermocline, while the zonal advective feedback mainly controls its decay. The quasi-decadal oscillation (QDO) tends to follow the 11-years solar cycle with a 1-to-2-year phase delay, meanwhile, it possibly links to the nonlinear behavior of ENSO. The cause of intensification of the QDO over the past 70 years, however, remains elusive.

Plain Language Summary The sea surface temperature (SST) at the equatorial central Pacific (ECP) exhibits a prominent 11-year periodicity over the last 70 years. This quasi-decadal oscillation (QDO) can significantly influence tropical cyclone activity and continental climate anomalies. This work provides a novel description of the QDO phenomenon as a prominent mode of SST variability in the subtropical North Pacific and equatorial central Pacific (ECP). The initial QDO warming develops over a northeast-southwestward elongated belt extending from California's off-coast to the ECP by the interaction between atmospheric heating-induced weakening trade winds and underlying SST anomalies. The amplification of ECP warming is primarily attributed to equatorward heat transport, while its decay is principally caused by the transport of cold water from the eastern Pacific. The QDO is found to follow the 11-year solar irradiance cycle with a 1-to-2-year phase delay and potentially link to the decadal variability of El Niño-Southern Oscillation. However, why the QDO has strengthened since the 1950s remains elusive.

1. Introduction

Pacific sea surface temperature (SST) variability has the most profound impacts on global climate variations. The Pacific basin-wide variability is dominated by El Niño-Southern Oscillation (ENSO) (Weare, 1982), Pacific Decadal Oscillation (PDO) (Mantua et al., 1997), North Pacific Gyre Oscillation (NPGO) (Di Lorenzo et al., 2008), and Interdecadal Pacific Oscillation (IPO) (Power et al., 1999) on various time scales. Besides these basin modes, a relatively weak quasi-decadal oscillation (QDO) was detected first by multi-taper frequency-domain singular value decomposition analysis of the localized variance spectrum of SST and sea-level pressure (SLP) (Allan, 2000; Allan et al., 2003; Brassington, 1997; Tourre et al., 2001). The quasi-decadal signals were also recognized to exist in the upper ocean temperature variability (White et al., 2003b), subsurface ocean temperature (Luo & Yamagata, 2001), Kuroshio extension jet intensity (Qiu, 2003), and the Pacific sea level (Lyu et al., 2017).

Observational studies found QDO and ENSO signals share similar spatial structure and relative phasing of SST and SLP anomalies, but QDO evolution is amplified from the northeast tropical Pacific into the central Pacific (e.g., Tourre et al., 2001), and the warmest SST anomalies displaced into the central-western equatorial Pacific (e.g., Allan, 2000). The majority of these studies are based on narrow band-pass filtered data, leading to exaggeratedly periodic QDO pattern. Thereby, the QDO is generally regarded as an extended Pacific ENSO signal, and its characteristic spatial structure and development are diluted. As such, the mechanisms that trigger and control the QDO evolution remain poorly understood.

The origins of the Pacific quasi-decadal variability remain controversial, involving both the internal dynamics and external forcing. The phase transition of the QDO was thought to be governed by an ENSO-like delayed action oscillation mechanism (Battisti & Hirst, 1989; Schopf & Suarez, 1988) in the tropical Pacific (White et al., 2003b; White & Liu, 2008a, 2008b). However, the QDO could trigger further poleward off-equatorial Rossby waves in the central tropical North Pacific (Capotondi & Alexander, 2001). On the other hand, observation and conceptual model results suggested that the Pacific QDO is modulated by the 11-years solar cycle (White et al., 2003a; White & Liu, 2008a, 2008b). Moreover, the decadal solar oscillation effects on the tropical Pacific have been explored widely. During the solar peak years, the intensified precipitation in the intertropical convergence zone and south Pacific convergence zone strengthens the Hadley and Walker circulations, increasing trade winds, enhancing equatorial ocean upwelling, and lowering eastern equatorial Pacific SSTs (Meehl et al., 2009; Van Loon et al., 2004, 2007). However, the cooling is significantly different from the La Niña event in the stratosphere structure (Van Loon & Meehl, 2008).

The QDO can significantly influence tropical cyclone activity and continental climate anomalies (Anderson et al., 2016; S. Wang et al., 2014). This study aims to address the following three questions: (a) What are the distinct spatial-temporal structure of Pacific QDO? (b) What physical processes control their development and decay? And (c) what factors set up the decadal time scale of the Pacific QDO?

2. Data

The monthly mean SST data are obtained from the Hadley Centre Sea Ice and Sea Surface Temperature (HadISST) (Rayner et al., 2003), and the National Oceanic and Atmospheric Administration Extended Reconstructed SST (ERSST) version 5 (Huang et al., 2017). To reduce each SST data set's uncertainty, we have made a "merged" monthly mean SST data set by simply taking their arithmetic means over 1871–2018. The ocean reanalysis data sets, including potential temperature, zonal and meridional currents, vertical velocity, and total downward heat flux at the surface, are derived from the Global Ocean Data Assimilation System (GODAS) with 0.33° latitude × 1° longitude grid for 1980–2018 (Behringer & Xue, 2004).

The monthly mean reanalysis data (including SLP, precipitation, and 1,000-hPa winds) were obtained by merging ERA-20C during 1900–1957 (Poli et al., 2013), ERA-40 during 1958–1978 (Uppala et al., 2005), and ERA-Interim during 1979–2018 (Dee et al., 2011) after removing the differences in monthly mean climatology during their respective overlapping periods.

The NOAA Climate Data Record (CDR) of Total Solar Irradiance (TSI), NRLTSI Version 2 is also used (https://data.nodc.noaa.gov/cgi-bin/iso?id=gov.noaa.ncdc:C00828).

3. Pacific QDO Index and its Characteristic Spatial-Temporal Structure

To detect the geographic locations where the SST variation has a significant quasi-decadal (9- to 13- year) signal, we conducted spectral analysis over each grid in the Pacific. The significant quasi-decadal signals are found primarily in a northeast-southwest tilted belt from the west coast of the United States to the equatorial Central Pacific (ECP) near the dateline (Figure S1). The ECP has the most prominent and season-independent decadal signal and is the action center of the Pacific QDO. For convenience, we define an ECP index by the mean SST anomalies averaged over (10°S-10°N, 165°E-165°W).

The power spectrum of the yearly-mean ECP index (Figure 1a) exhibits a conspicuous 11-year periodicity during 1951–2018 (Figure 1b). This 11-year peak is also seen from the interannual variation of each seasonal mean SST anomalies, i.e., March-April-May (MAM), June-July-August (JJA), September-October-November

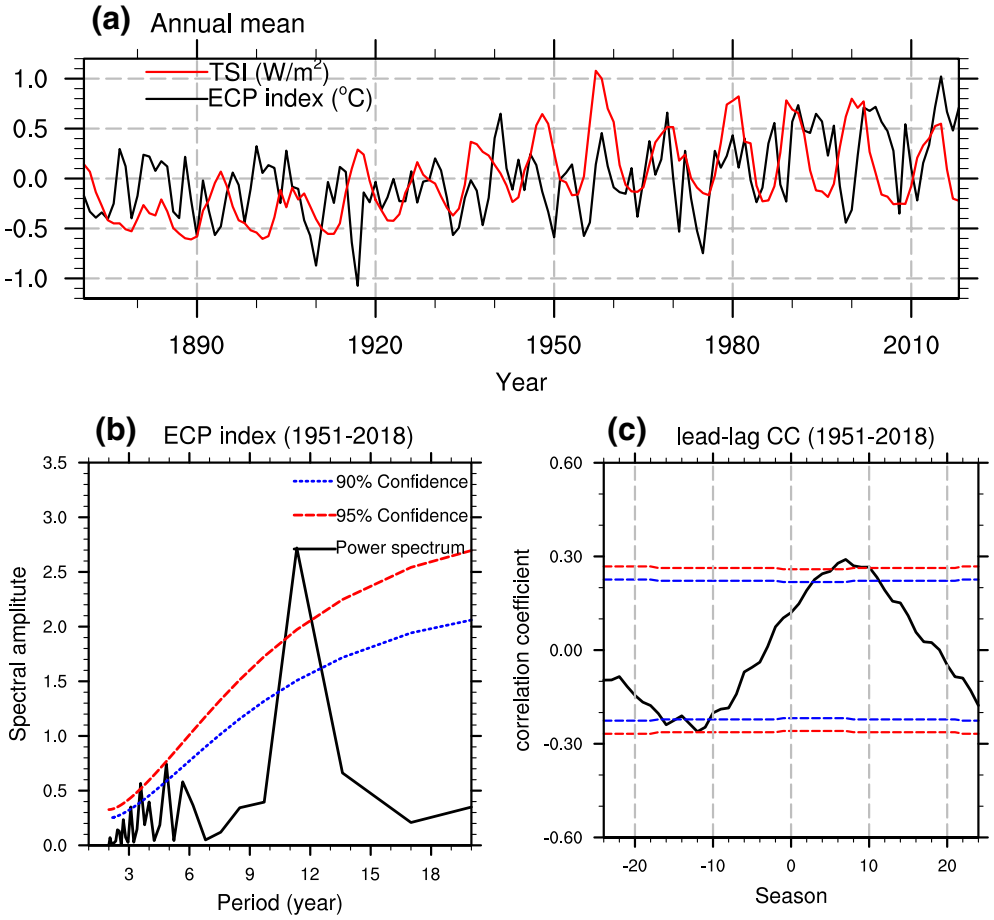

Figure 1. (a) Time series of the annual mean SST index (°C) and TSI (W/m^2) during 1871–2018. The ECP index is defined as the SST anomaly averaged over the region (10°S-10°N, 165°E-165°W). (b) Power spectrum of the annual mean ECP index during 1951–2018. The blue (red) curve represents the upper bound of the Markov red noise spectrum at the 90% (95%) confidence level. (c) Lead-lag correlation coefficient between the seasonal mean ECP index and seasonal mean TSI during 1951–2018. The blue (red) lines indicate statistical significance at the 90% (95%) confidence level with the effective degrees of freedom ranging from 52 to 57 (Bretherton et al., 1999). A positive value for the season in (c) means TSI leads ECP index. Un-detrended SST data were used. ECP, equatorial central Pacific; TSI, total solar irradiance.

(SON), and December-January-February (DJF), suggesting that the QDO exists throughout the seasonal cycle (Figure S2). The index can be used to represent the Pacific QDO, which is also referred to as the QDO index hereafter.

Can the QDO be seen in a long record? We find that the quasi-decadal peak is absent during 1871–1950 (Figure S3). This absence might be affected by the degraded quality of the SST data, but it likely suggests the nonstationary nature of the QDO. Given the QDO phenomenon has become significant after the 1950s, our analysis will focus on the past 70 years.

To depict coherent QDO structure and to find how a QDO warm event evolves, we first use the annual mean, detrended data to construct the lead-lag correlation maps with reference to the yearly mean QDO index from the −3 to +3 years (Figure 2 and Figure S4). Note that the lead-lag regression maps show essentially the same evolution processes as shown by the lead-lag regression maps (Figure S5).

During the transition phases (-3 and +3 years), the significant SST anomalies are almost absent, suggesting that the warming looks like an episodic event (Fig. S4). This view is different from the previous results that used narrowly bandpass-filtered data, which showed a cyclic-like event with significant continuing signals in the transition phases (e.g., Tourre et al., 2001).

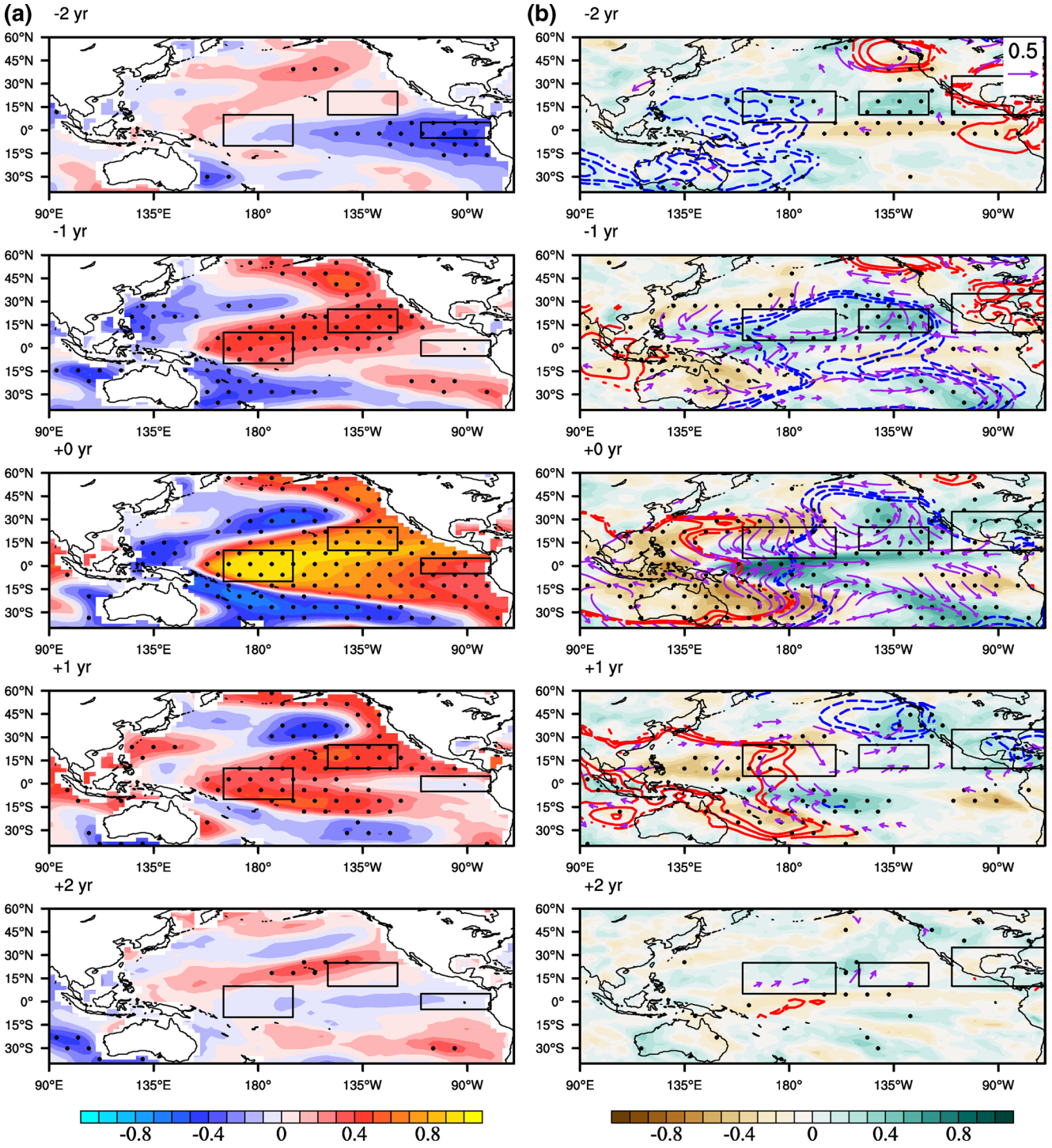

Figure 2. Evolution of the Pacific Quasi-Decadal Oscillation (QDO). Shown are the lead-lag correlation maps of the yearly mean anomalies of (a) SST, (b) precipitation (color), SLP (contour), and 1,000-hPa winds (vectors) with reference to the annual mean ECP index during 1951–2018 from −2 years to +2 years. The dotted areas denote significance at the 90% confidence level, which is conducted by a two-tailed *t*-test, in (a) for SST and in (b) for precipitation. The red solid (blue dashed) lines represent the positive (negative) pressure, the contour interval is 0.05, and only the contours and vectors significant at a 90% confidence level are shown in (b). The black boxes show the key locations used in Figure 3. SLP, sea-level pressure.

Two years before the QDO peak warming, a significant cooling is seen in the eastern equatorial Pacific coupled with an SLP seesaw with an anomalous low over the western Pacific and an anomalous high over Central America (Figure 2). The eastern Pacific cooling generates northward flow and increases precipitation in the subtropical eastern North Pacific (ENP) (10°N-25°N, 150°W-120°W), followed by significant warming over the Gulf of Alaska and a northeast-southwestward tilted warming belt from Baja California to the ECP at −1 year (Figure 2). The QDO warming then rapidly amplifies at the ECP and reaches its peak at year 0 with a mega-El Niño-like pattern (Wang et al., 2013a).

However, different from El Niño, the warming develops from the tropical-subtropical North Pacific rather than along the equator; besides, the maximum warming occurs near the dateline (160°E-160°W) and the SLP seesaw anomalies are equatorially symmetric rather than biased to the southern hemisphere (SH) as in ENSO. The off-equatorial triangle warming resembles a PDO pattern, but a notable equatorial asymmetry is seen in the eastern Pacific with enhanced warming along the northern hemisphere (NH) ITCZ.

The QDO warming rapidly decays along the equator after the peak. From +1 to +2 years, the SH warming disappears while a remnant NH warming remains visible. Notably, the equatorial eastern Pacific (EEP) cooling is absent in the QDO decay phase, indicating a development-decay asymmetry and an NH-SH asymmetry in the Pacific QDO life cycle. The development and decay processes seem to feature a standing expansion/retraction without apparent propagation of the SST anomaly. Thus, Pacific QDO appears to be a standing oscillation.

Note that Figure 2 is made of yearly mean data, which does not fully filter interannual variability. To further remove the ENSO signals, we used 3-years running mean data to present the QDO evolution (Figure S6). The evolution shown in Figure S6 resembles, to a large extent, the evolution shown in Figure 2, suggesting that the QDO evolution shown in Figure 2 is robust. But, by removal of the ENSO signals, the warming in the equatorial far eastern Pacific disappears, suggesting that QDO is more concentrated in the central Pacific.

4. Initiation and Development Mechanisms of the QDO Warming

Where does the ECP warming originate? How is the warming triggered? To address these questions, we have to examine the seasonal mean evolutions. Based on Figure 2, we select several air-sea interaction variables at various QDO active locations to examine their time evolutions and lead-lag relationships (Figure 3).

The earliest precursor that preludes the ECP warming is the significantly positive SLP anomalies over Central-North America at −10 season (Figure 3a), which, by generating equatorial easterly anomalies, favors the EEP cooling that peaks in −8 and −7 seasons (Figure 3b). Meanwhile, the EEP cooling enhances the subtropical ENP (10°N-25°N, 150°W-120°W) precipitation, which starts at −7 season and reaches its peak around −5 season (Figure 3c). The chain scenarios from Figure 3a to 3c suggest that the central-North American rising pressure and EP cooling triggers the initial development of the ENP precipitation.

The enhanced ENP precipitation is followed by decreasing pressure in the subtropical central North Pacific (CNP, 5°N-25°N, 160°E-160°W) (Figure 3d). With the deepening of the anomalous CNP low, the climatological northeasterly trade winds weaken, as shown by the negative wind speed anomalies around −5 and −4 season (Figure 3e). The weakened trades lead to rapid warming in the ENP, as evidenced by the maximum SST tendency at −4 season (Figure 3e).

The chain scenarios from Figure 3c to 3e, suggest that the development of QDO warming in the subtropical NP may involve positive atmosphere-ocean feedback. This positive feedback is characterized by the atmospheric heating-induced Rossby wave response and associated dipolar SST anomalies (warming to the southeast and cooling to the northwest of the Rossby low) (Wang et al., 2000; Wang et al., 2013b). As shown in Figure 2 (panel −1 year), to the southeast of the cyclonic (low-pressure) anomalies, the weakened trades-reduced evaporation and entrainment cooling induce sea surface warming. On the other hand, the southwestward tilted warming belt from Baja California to the ECP enhances moisture convergence and precipitation heating that, in turn, generates ascending Rossby-wave low to strengthen the cyclonic anomaly during the westward propagation of the Rossby waves.

Of interest is that while the ENP and ECP warming is nearly simultaneous (Figure 3f), the initial warming at the ENP occurs earlier than ECP, suggesting the QDO warming may extend from ENP southwestward

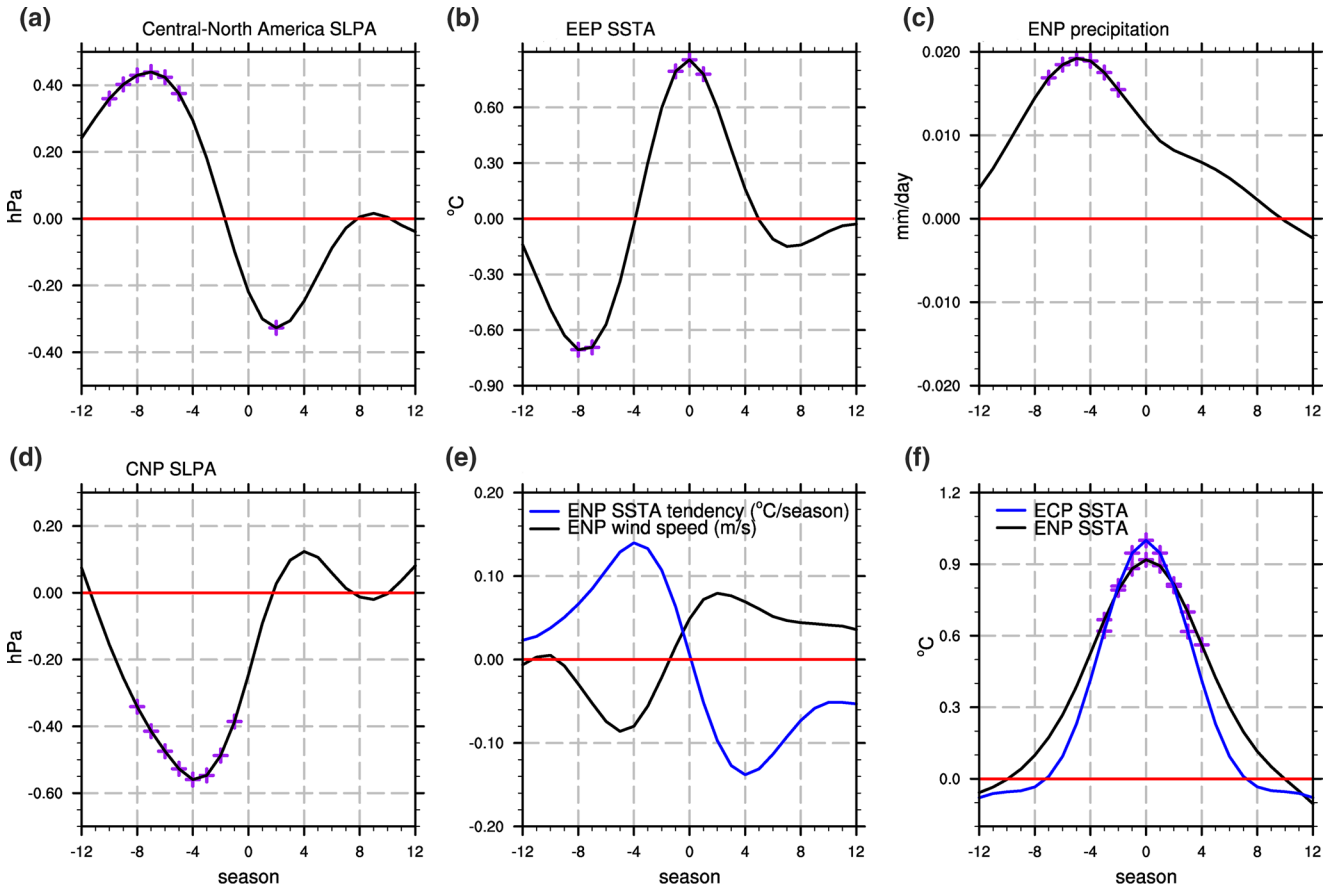

Figure 3. Evolutions of the regressed variables at various key locations with reference to the ECP index from −12 to +12 season with zero denoting the ECP peak warming: (a) Central-North America (10°N-35°N, 110°W-70°W) SLP anomalies (hPa), (b) the EEP (5°S-5°N, 110°W-80°W) SST anomalies (°C), (c) the subtropical eastern North Pacific (ENP, 10°N-25°N, 150°W-120°W) precipitation anomalies (mm/day), (d) the subtropical central North Pacific (CNP, 5°N-25°N, 160°E-160°W) SLP anomalies (hPa), (e) the ENP wind speed anomalies (m/s) and the ENP SST tendency (°C/month), and (f) the ENP and the ECP SST anomalies (°C). To better focus on decadal signals, all seasonal-mean detrended variables and the ECP index are smoothed by a 5-season running mean. The purple crosses shown in each panel indicate the values that are statistical significance at the 90% confidence level, which is obtained by a two-tailed *t*-test. ECP, equatorial central Pacific; EEP, equatorial eastern Pacific; ENP, eastern North Pacific; SLP, sea-level pressure; SST, sea surface temperature.

to the ECP. Note also that the ENP warming decays slower than the ECP, meaning that the decay of QDO warming may extend from ECP northeastward to ENP.

5. Equatorial Feedback Mechanisms for the Amplification and Decay of ECP Warming

The ECP's fastest-warming and cooling occur around the −4 and +4 seasons (Figure 3f). To reveal coupled dynamic processes involving in the evolution of the QDO over the ECP, we conducted an ocean mixed layer heat budget analysis (Text S1). Due to the limitation of GODAS data, the analysis is only made for 1980–2018. The diagnosed temperature tendency (Sum, 0.075 °C/month) is generally consistent with the observed tendency (0.093 °C/month) in the development stage (−5 to −3 season) (Table 1). The nonlinear term is negligibly small, and the surface heat flux tends to damp the warming during both the development and decay stages.

The rapid amplification of ECP warming is mainly attributed to the meridional heat advection by mean (0.039 °C/month) and anomalous currents (0.026 °C/month), and the vertical advection of anomalous temperature by mean upwelling (0.037 °C/month). The two zonal advective terms tend to offset each other, contributing little to the ECP warming. In contrast, the ECP warming decay is primarily controlled by the zonal heat advection (−0.130°C/month) and augmented by the vertical advection by mean upwelling due to

Table 1
Ocean Mixed Layer Heat Budget Analysis for the Development and Decay Stages of the QDO Over the Equatorial Central Pacific (5°S-5°N, 165°E-165°W).

	$-\frac{u'\partial\overline{T}}{\partial x}$	$-\frac{\overline{u}\partial T'}{\partial x}$	$-\frac{v'\partial\overline{T}}{\partial y}$	$-\frac{\overline{v}\partial T'}{\partial y}$	$-\frac{w'\partial\overline{T}}{\partial z}$	$-\frac{\overline{w}\partial T'}{\partial z}$	NL	$\frac{Q'}{\rho C_p H}$	Sum	$\frac{\partial T'}{\partial t}$
Development stage	0.017	−0.024	**0.026**	**0.039**	−0.008	**0.037**	0.000	−0.013	0.075	0.093
Decay stage	**−0.130**	0.046	0.040	0.019	0.010	**−0.030**	0.005	−0.012	−0.053	−0.098

The regressed anomalies with reference to the ECP index are used in the heat budget computation during the development stage (mean of −5 season to −3 season) and decay stage (mean of the +3 to +5 season). Sum means the estimated temperature tendency. Nonlinear (NL) term is the sum of the $-\frac{u'\partial T'}{\partial x}, -\frac{v'\partial T'}{\partial y}, -\frac{w'\partial T'}{\partial z}$. The units are °C/month. The dominant feedbacks in the development and decay of ECP warming are marked bold.

thermocline feedback (−0.030°C/month). The processes governing ECP warming contrasts the central Pacific El Niño development in which zonal heat advection dominates (Kug et al., 2009; B. Wang et al., 2019).

To qualitatively illustrate the major terms' contribution in the ECP SSTA development and decay stages, we present a schematic diagram (Figure 4) with the highlight as follows. The climatological mean thermal state of the ECP mixed layer is characterized by (a) negative (westward) zonal temperature gradients (-4.0×10^{-4}°C/Km), (b) positive (upward) vertical temperature gradients (6.2°C/Km), and (c) poleward meridional temperature gradients (positive in the NH 6.7×10^{-4}°C/Km while negative in the SH, -1.5×10^{-3}°C/Km) as illustrated by the color shading. The climatological mean circulation is dominated by the averaged westward currents (−9.2 cm/s), poleward meridional currents (3.2 cm/s in the NH, and −2.5 cm/s in the SH), and upwelling (2.8×10^{-6} m/s) as illustrated by the green arrows. Because of the equatorially symmetric feature of the meridional advection, only the NH part of the meridional temperature advection is discussed.

Anomalous quantities are qualitatively illustrated in the figure except the upwelling as its heat advection is negligibly small (Table 1). During the amplification stage (Figure 4a), three main processes contribute to the rapidly rising SST. The first is the anomalous southward meridional currents ($v'<0$) in the NH that transports mean-state warmer seawater equatorward, contributing to ECP warming. The second contributor is the mean northward currents that transport anomalously cooler water ($\partial T' / \partial y < 0$) away from the equator, reducing the heat loss by the northward mean currents' advection and enhancing the ECP warming. The third is the mean upwelling that transport anomalously warm water ($\partial T' / \partial z < 0$), reducing the cooling advected by the mean upwelling and increasing ECP SST. The negative anomalous vertical temperature gradient is mainly due to a deepening thermocline associated with the mixed layer currents convergence. During the decay stage of the QDO, the predominant contributor is the anomalous westward currents that transport cold water from the east to cool the ECP ocean mixed layer.

6. Discussion: What Determines the Time Scale of the QDO?

We present relevant evidence to support two hypotheses.

6.1. The 11-Year Solar Irradiance Forcing

The appealing aspect of the solar forcing hypothesis is to explain the time scale of QDO. The TSI shows a significantly increasing trend since 1871, and the intensity of the TSI variation was amplified to about 0.5 W/m^2 around 1950 (Figure 1a). During 1951–2018, the TSI cycle tends to lead the QDO by six (4–10) seasons (Figure 1c), i.e., the Central Pacific reaches a peak warming about 1–2 years after the maximum solar irradiance. However, the lead-lag correlation coefficient between the QDO and TSI is not significant during 1871–1950, conceivably due to the weak 11-year solar forcing (Figure 1a) as speculated by White (2006) and White et al. (1998).

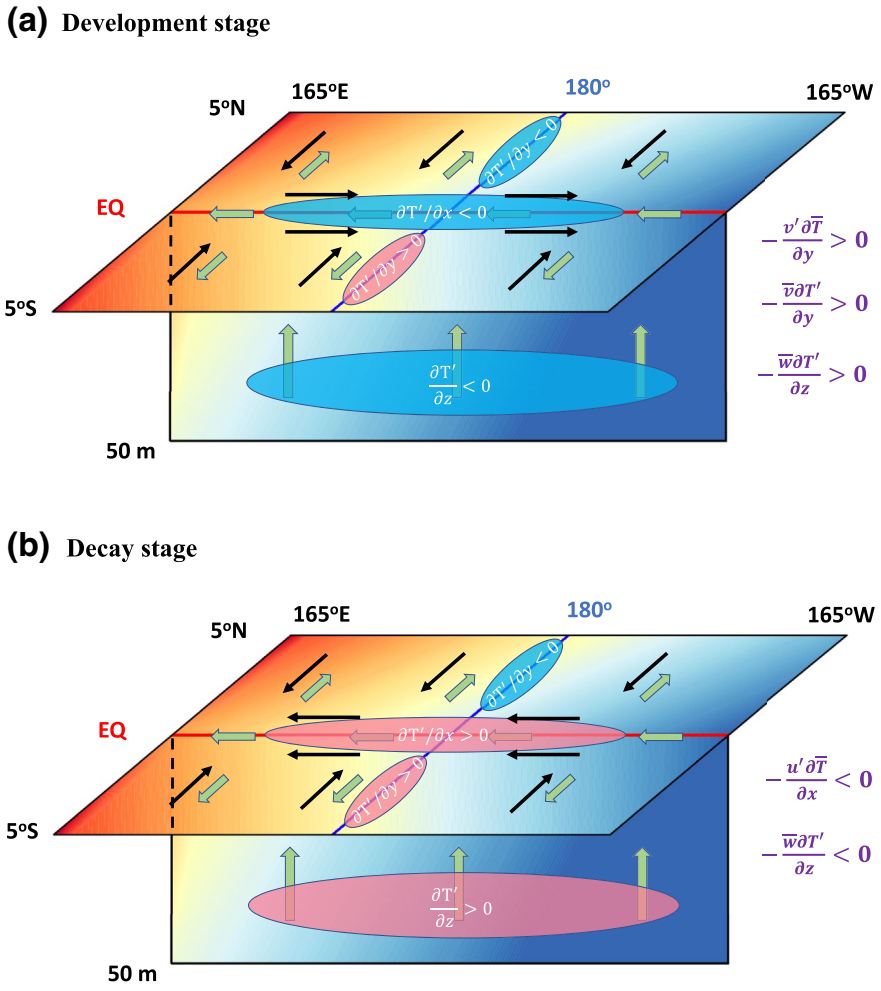

Figure 4. Schematic diagram illustrating major processes responsible for the ECP (5°S-5°N, 165°E-165°W) warming's development and decay. The red (blue) color donates the warm (cold) mean temperature. Green vectors denote the area- and vertically averaged climatological mean currents and vertical motion in the ECP mixed layer. The black vectors illustrate the anomalous currents, the orange (blue) ellipse shading represents the positive (negative) anomalous SST gradients. The terms on the right-hand-side of each panel indicates major terms that contribute to the development (a) and decay (b) of ECP warming. The sign of each term is based on the diagnosed results over the ECP region during 1980–2018 derived from the GODAS data. ECP, equatorial central Pacific; SST, sea surface temperature.

The problematic aspect of the solar forcing hypothesis is to establish a cause-effect relationship. Previous studies have shown that a weak La Niña-like response occurs during the 11-year solar cycle peak followed by a Central Pacific El Niño-like response 1−2 years later (Meehl & Arblaster, 2009; Misios et al. 2016, 2019). By analyzing the SST and SLP anomalies with reference to the composite TSI peak years (1957, 1968, 1979, 1989, 2000, and 2014), we find that a La Niña condition occurs one year before the solar peak (Figure S7). At the solar peak, an anomalous low (cyclone) developed in the subtropical NP, reducing the northeasterly trade wind, resulting in ENP warming. One year after the solar peak, ECP warming reaches its maximum. Phenomenologically, the evolution of anomalies associated with the TSI resembles that of QDO except with a one-year lead, suggesting that the QDO might be a response to the 11-year solar cycle. The solar forcing may induce QDO by triggering the eastern Pacific cooling. Besides, the subtropical ocean is an enormous heat reservoir; thereby, the impacts of the enhanced solar forcing may be 'memorized' by the ocean. However, the precise processes that link the TSI and QDO remain elusive.

6.2. Low-Frequency Variability of ENSO

An alternative hypothesis is that the ENSO's complex nonlinear property may contribute to the preferred time scale of QDO. The activity center of QDO is located in a "buffer" zone between the cold tongue and warm pool. The ECP SST variability is necessarily affected by ENSO, but not totally. ENSO variability is measured by the Oceanic Niño Index (ONI), the SST anomalies averaged over the NINO 3.4 region (5°S-5°N, 170°W-120°W). We find that the annual mean ONI shows a significant 11-years peak during 1951–2018 and a 9-years peak during 1871–1950 (Figure S8), suggesting that ENSO has an "intrinsic" quasi-decadal time scale. During 1951–2018, the annual mean ONI and QDO are highly correlated with R = 0.81 (n = 56, $p < 0.01$). The six QDO peak warming years (1958, 1969, 1980, 1992, 2003, and 2015, Figure 1) tend to concur with two-year El Niño (68–69, 14–15) or clustering El Niño (91–94, 02–04), whereas the six QDO minima (1955, 1964, 1974, 1985, 1999, and 2011) tend to be in phase with the 2–3-year La Niña events including 1954–1956, 1973–1975, 1984–1985, 1998–2000, and 2010–2011. Both the clustering El Niño or consecutive La Niña and El Niño may be related to the nonlinear El Niño- La Niña amplitude asymmetry and development-decay asymmetry. However, it is unclear whether the random ENSO nonlinearity generates QDO or QDO modulates ENSO, causing consecutive La Niña or clustering El Niño events.

7. Summary

It has been difficult to describe the defining features of Pacific QDO because ENSO, PDO, and IPO dominate the Pacific SST variability whereas QDO cannot be clearly identified on the basin scale. This work describes QDO as a distinct regional mode of SST variability in the tropical North Pacific and explains the coupled dynamics responsible for its characteristic evolution.

We find that the QDO is a nonstationary phenomenon with an eye-catching 11-year periodicity during 1951–2018 but not during 1871–1950. The ECP warming appears to be an episodic-like and quasi-standing event, originated in a northeast-southwest tilted belt from the west coast of the United States to the ECP. QDO warming development involves both positive feedback between atmospheric heating-induced Rossby waves and underlying SST in the tropical North Pacific and equatorial meridional advective and thermocline feedback. In contrast, the decay of warming relies on zonal advective feedback. The QDO dynamics distinguish from ENSO dynamics. The QDO warming develops in the subtropical North Pacific by off-equatorial atmosphere-ocean interaction rather than along the equator as in ENSO, and the amplification of ECP warming mainly due to meridional heat advection, not the zonal advection feedback as in ENSO.

The decadal time scale of the QDO might be regulated by the 11-year solar cycle and/or the nonlinear behavior of ENSO. The first is hinted by the fact that QDO lags TSI by 1-to-2 years and the maximum TSI seems to trigger the subtropical North Pacific warming of QDO. The latter is implied by the relationship between the clustering El Niño or persisting La Niña. The two hypotheses are distinctive but not mutually exclusive. However, the precise physical processes that determine the quasi-decadal time scale remain to be established.

In addition to the origin of the QDO time scale, several other issues call for future investigation. The main question to be addressed is what has caused the Pacific QDO strengthening after 1950. Is the strengthening related to the enhanced 11-year solar cycle or other factors, especially the increasing greenhouse gas forcing? The QDO, the prominent mode of the SST variability in the equatorial central Pacific, involves a sequence of air-sea interaction in the subtropical North Pacific. Therefore, QDO's off-equatorial SST patterns in the developing stage (−3, −1, and 0 years) resemble those of two leading modes of the North Pacific decadal variability, i.e., NPGO (Di Lorenzo et al., 2008) and the Pan-Pacific Decadal variation mode or PDO (Nigam et al., 2020). However, the QDO also involves the equatorial coupled dynamics on the decadal time scale. The QDO primarily involves variability in the equatorial central Pacific and subtropical North Pacific and linkage with South Pacific through the ECP teleconnection. On the other hand, the PDO and NPGO involve more variabilities and processes in the subarctic-midaltitude North Pacific. Previous studies have also shown that the Atlantic variability may trigger the PDO-like SST pattern (Gong et al., 2020; Johnson et al., 2020; Yang et al., 2020; Zhang & Delworth, 2007). Therefore, the linkages between the QDO and the tropical inter-ocean basin interactions require further investigation. Besides, given the critical location of the QDO, its impacts on tropical and global climate variations deserve in-depth exploration.

Data Availability Statement

Data related to this paper can be downloaded from the following.
ECMWF reanalysis, https://www.ecmwf.int/en/forecasts/datasets/browse-reanalysis-datasets
HadISST, https://www.metoffice.gov.uk/hadobs/hadisst/
ERSST, https://www.ncdc.noaa.gov/data-access/marineocean-data/extended-reconstructed-sea-surface-temperature-ersst-v5.
GODAS ocean reanalysis data sets, https://psl.noaa.gov/data/gridded/data.godas.html
NOAA Climate Data Record (CDR) of Total Solar Irradiance (TSI), NRLTSI Version 2, https://data.nodc.noaa.gov/cgi-bin/iso?id = gov.noaa.ncdc:C00828.

Acknowledgments
This work was supported by the National Key Research and Development Program of China (Grant No. 2016YFA0600401) and the National Natural Science Foundation of China (Grant Nos. 41971108, 41420104002, 42075049, 41671197, and 41971021). B. Wang acknowledges the support of NSF/Climate Dynamics Award #AGS-1540783. C. -H. Jin acknowledges the support from the program of China Scholarships Council (No. 201806860029). This is publication No. 11204 of the School of Ocean and Earth Science and Technology, publication No. 1492 of the International Pacific Research Center and publication No. 339 of the Earth System Modeling Center.

References

Allan, R. J. (2000). ENSO and climatic variability in the last 150 years. In H. F. Diaz, & V. Markgraf (Eds.), *El Niño and the southern oscillation: Multiscale variability, global and regional impacts* (pp. 3–55). Cambridge: Cambridge University Press.
Allan, R. J., Reason, C. J. C., Lindesay, J. A., & Ansell, T. J. (2003). Protracted'ENSO episodes and their impacts in the Indian Ocean region. *Deep Sea Research Part II: Topical Studies in Oceanography*, *50*(12–13), 2331–2347.
Anderson, B. T., Gianotti, D. J. S., Furtado, J. C., & Di Lorenzo, E. (2016). A decadal precession of atmospheric pressures over the North Pacific. *Geophysical Research Letters*, *43*(8), 3921–3927. https://doi.org/10.1002/2016GL068206
Battisti, D. S., & Hirst, A. C. (1989). Interannual variability in a tropical atmosphere–ocean model: Influence of the basic state, ocean geometry and nonlinearity. *Journal of the Atmospheric Sciences*, *46*(12), 1687–1712.
Behringer, D. W., & Xue, Y. (2004). Evaluation of the global ocean data assimilation system at NCEP: The Pacific Ocean. *Proceedings of the eighth symposium on integrated observing and assimilation systems for atmosphere, oceans, and land surface* AMS 84th Annual Meeting, Washington State Convention and Trade Center.
Brassington, G. B. (1997). The modal evolution of the southern oscillation. *Journal of Climate*, *10*(5), 1021–1034.
Bretherton, C. S., Widmann, M., Dymnikov, V. P., Wallace, J. M., & Bladé, I. (1999). The effective number of spatial degrees of freedom of a time-varying field. *Journal of Climate*, *12*(7), 1990–2009.
Capotondi, A., & Alexander, M. A. (2001). Rossby waves in the tropical North Pacific and their role in decadal thermocline variability. *Journal of Physical Oceanography*, *31*(12), 3496–3515.
Dee, D. P., Uppala, S. M., Simmons, A. J., Berrisford, P., Poli, P., Kobayashi, S., et al. (2011). The ERA-Interim reanalysis: Configuration and performance of the data assimilation system. *Quarterly Journal of the Royal Meteorological Society*, *137*(656), 553–597.
Di Lorenzo, E., Schneider, N., Cobb, K. M., Franks, P. J. S., Chhak, K., Miller, A. J., et al. (2008). North Pacific Gyre Oscillation links ocean climate and ecosystem change. *Geophysical Research Letters*, *35*(8), L08607. https://doi.org/10.1029/2007GL032838
Gong, Z., Sun, C., Li, J., Feng, J., Xie, F., Ding, R., et al. (2020). An inter-basin teleconnection from the North Atlantic to the subarctic North Pacific at multidecadal time scales. *Climate Dynamics*, *54*(1–2), 807–822.
Huang, B., Thorne, P. W., Banzon, V. F., Boyer, T., Chepurin, G., Lawrimore, J. H., et al. (2017). Extended reconstructed Sea surface temperature, version 5 (ERSSTv5): Upgrades, validations, and intercomparisons. *Journal of Climate*, *30*(20), 8179–8205.
Johnson, Z. F., Chikamoto, Y., Wang, S. S., McPhaden, M. J., & Mochizuki, T. (2020). Pacific decadal oscillation remotely forced by the equatorial Pacific and the Atlantic Oceans. *Climate Dynamics*.*55*(3-4), 789–811. https://doi.org/10.1007/s00382-020-05295-2
Kug, J.-S., Jin, F.-F., & An, S.-I. (2009). Two types of El Niño events: Cold tongue El Niño and warm pool El Niño. *Journal of Climate*, *22*(6), 1499–1515.
Luo, J., & Yamagata, T. (2001). Long-term El Niño-southern oscillation (ENSO)-like variation with special emphasis on the south Pacific. *Journal of Geophysical Research*, *106*(C10), 22211–22227.
Lyu, K., Zhang, X., Church, J. A., Hu, J., & Yu, J.-Y. (2017). Distinguishing the quasi-decadal and multidecadal sea level and climate variations in the Pacific: Implications for the ENSO-like low-frequency variability. *Journal of Climate*, *30*(13), 5097–5117.
Mantua, N. J., Hare, S. R., Zhang, Y., Wallace, J. M., & Francis, R. C. (1997). A Pacific interdecadal climate oscillation with impacts on salmon production. *Bulletin of the American Meteorological Society*, *78*(6), 1069–1080.
Meehl, G. A., & Arblaster, J. M. (2009). A lagged warm event-like response to peaks in solar forcing in the Pacific region. *Journal of Climate*, *22*(13), 3647–3660.
Meehl, G. A., Arblaster, J. M., Matthes, K., Sassi, F., & Van Loon, H. (2009). Amplifying the Pacific climate system response to a small 11-year solar cycle forcing. *Science*, *325*(5944), 1114–1118.
Misios, S., Gray, L. J., Knudsen, M. F., Karoff, C., Schmidt, H., & Haigh, J. D. (2019). Slowdown of the Walker circulation at solar cycle maximum. *Proceedings of the National Academy of Sciences*, *116*(15), 7186–7191. https://doi.org/10.1073/pnas.1815060116
Misios, S., Mitchell, D. M., Gray, L. J., Tourpali, K., Matthes, K., Hood, L., et al. (2016). Solar signals in CMIP-5 simulations: Effects of atmosphere–ocean coupling. *Quarterly Journal of the Royal Meteorological Society*, *142*(695), 928–941.
Nigam, S., Sengupta, A., & Ruiz-Barradas, A. (2020). Atlantic–Pacific links in observed multidecadal SST variability: Is the Atlantic multidecadal oscillation's phase reversal orchestrated by the Pacific decadal oscillation?. *Journal of Climate*, *33*(13), 5479–5505.
Poli, P., Hersbach, H., Tan, D., Dee, D., Thepaut, J.-N., Simmons, A., et al. (2013). *The data assimilation system and initial performance evaluation of the ECMWF pilot reanalysis of the 20th-century assimilating surface observations only (ERA-20C)*, Shinfield Park, Reading, UK: European Centre for Medium Range Weather Forecasts.
Power, S., Casey, T., Folland, C., Colman, A., & Mehta, V. (1999). Inter-decadal modulation of the impact of ENSO on Australia. *Climate Dynamics*, *15*(5), 319–324.
Qiu, B. (2003). Kuroshio Extension variability and forcing of the Pacific decadal oscillations: Responses and potential feedback. *Journal of Physical Oceanography*, *33*(12), 2465–2482.
Rayner, N. A. A., Parker, D. E., Horton, E. B., Folland, C. K., Alexander, L. V., Rowell, D. P., et al. (2003). Global analyses of sea surface temperature, sea ice, and night marine air temperature since the late nineteenth century. *Journal of Geophysical Research*, *108*(D14), 4407. https://doi.org/10.1029/2002JD002670
Schopf, P. S., & Suarez, M. J. (1988). Vacillations in a coupled ocean-atmosphere model. *Journal of the Atmospheric Sciences*, *45*(3), 549–566.

Tourre, Y. M., Rajagopalan, B., Kushnir, Y., Barlow, M., & White, W. B. (2001). Patterns of coherent decadal and interdecadal climate signals in the Pacific basin during the 20th century. *Geophysical Research Letters*, *28*(10), 2069–2072.

Uppala, S. M., Kållberg, P. W., Simmons, A. J., Andrae, U., Bechtold, V. D. C., Fiorino, M., et al. (2005). The ERA-40 re-analysis. *Quarterly Journal of the Royal Meteorological Society*, *131*(612), 2961–3012.

Van Loon, H., & Meehl, G. A. (2008). The response in the Pacific to the sun's decadal peaks and contrasts to cold events in the Southern Oscillation. *Journal of Atmospheric and Solar-Terrestrial Physics*, *70*(7), 1046–1055.

Van Loon, H., Meehl, G. A., & Arblaster, J. M. (2004). A decadal solar effect in the tropics in July–August. *Journal of Atmospheric and Solar-Terrestrial Physics*, *66*(18), 1767–1778.

Van Loon, H., Meehl, G. A., & Shea, D. J. (2007). Coupled air-sea response to solar forcing in the Pacific region during northern winter. *Journal of Geophysical Research*, *112*(D2), D02018. https://doi.org/10.1029/2006JD007378

Wang, S., Hakala, K., Gillies, R. R., & Capehart, W. J. (2014). The Pacific quasi-decadal oscillation (QDO): An important precursor toward anticipating major flood events in the Missouri River Basin?. *Geophysical Research Letters*, *41*(3), 991–997.

Wang, B., Liu, J., Kim, H.-J., Webster, P. J., Yim, S.-Y., & Xiang, B. (2013). Northern Hemisphere summer monsoon intensified by mega-El Niño/southern oscillation and Atlantic multidecadal oscillation. *Proceedings of the National Academy of Sciences*, *110*(14), 5347–5352.

Wang, B., Luo, X., Yang, Y.-M., Sun, W., Cane, M. A., Cai, W., et al. (2019). Historical change of El Niño properties sheds light on future changes of extreme El Niño. *Proceedings of the National Academy of Sciences*, *116*(45), 22512–22517. https://doi.org/10.1073/pnas.1911130116

Wang, B., Wu, R., & Fu, X. (2000). Pacific–East Asian teleconnection: How does ENSO affect east Asian climate?. *Journal of Climate*, *13*(9), 1517–1536.

Wang, B., Xiang, B., & Lee, J.-Y. (2013). Subtropical high predictability establishes a promising way for monsoon and tropical storm predictions. *Proceedings of the National Academy of Sciences*, *110*(8), 2718–2722.

Weare, B. C. (1982). El Nino and tropical Pacific ocean surface temperatures. *Journal of Physical Oceanography*, *12*(1), 17–27.

White, W. B. (2006). Response of tropical global ocean temperature to the Sun's quasi-decadal UV radiative forcing of the stratosphere. *Journal of Geophysical Research*, *111*(C9), C09020. https://doi.org/10.1029/2004JC002552

White, W. B., Cayan, D. R., & Lean, J. (1998). Global upper ocean heat storage response to radiative forcing from changing solar irradiance and increasing greenhouse gas/aerosol concentrations. *Journal of Geophysical Research*, *103*(C10), 21355–21366.

White, W. B., Dettinger, M. D., & Cayan, D. R. (2003a). Sources of global warming of the upper ocean on decadal period scales. *Journal of Geophysical Research: Oceans*, *108*(C8), 3248. https://doi.org/10.1029/2002JC001396

White, W. B., & Liu, Z. (2008a). Non-linear alignment of El Nino to the 11-yr solar cycle. *Geophysical Research Letters*, *35*(19), L19607. https://doi.org/10.1029/2008GL034831

White, W. B., & Liu, Z. (2008b). Resonant excitation of the quasi-decadal oscillation by the 11-year signal in the Sun's irradiance. *Journal of Geophysical Research*, *113*(C1), C01002. https://doi.org/10.1029/2006JC004057

White, W. B., Tourre, Y. M., Barlow, M., & Dettinger, M. (2003b). A delayed action oscillator shared by biennial, interannual, and decadal signals in the Pacific Basin. *Journal of Geophysical Research: Oceans*, *108*(C3), 3070. https://doi.org/10.1029/2002JC001490

Yang, Y.-M., An, S.-I., Wang, B., & Park, J. H. (2020). A global-scale multidecadal variability driven by Atlantic multidecadal oscillation. *National Science Review*, *7*(7), 1190–1197.

Zhang, R., & Delworth, T. L. (2007). Impact of the Atlantic multidecadal oscillation on North Pacific climate variability. *Geophysical Research Letters*, *34*(23), L23708. https://doi.org/10.1029/2007GL031601